ARTICLE

BIOTECHNOLOGY and BIOENGINEERING

Ion Exchange Chromatography of Antibody Fragments

Anders Ljunglöf,[1] Karol M. Lacki,[1] Jay Mueller,[2] Chithkala Harinarayan,[2] Robert van Reis,[2] Robert Fahrner,[2] James M. Van Alstine[1]

[1]GE Healthcare, Bio-Sciences AB, SE-751 84 Uppsala, Sweden;
telephone: +46 18 612 0000; fax: +46 18 612 1844; e-mail: Anders.Ljunglof@ge.com
[2]Genentech, Inc., 1 DNA Way, South San Francisco, California, 94080-4990

Received 31 March 2006; accepted 30 June 2006
Published online 9 November 2006 in Wiley InterScience (www.interscience.wiley.com). DOI 10.1002/bit.21124

ABSTRACT: Effects of pH and conductivity on the ion exchange chromatographic purification of an antigen-binding antibody fragment (Fab) of pI 8.0 were investigated. Normal sulfopropyl (SP) group modified agarose particles (SP Sepharose™ Fast Flow) and dextran modified particles (SP Sepharose XL) were studied. Chromatographic measurements including adsorption isotherms and dynamic breakthrough binding capacities, were complemented with laser scanning confocal microscopy. As expected static equilibrium and dynamic binding capacities were generally reduced by increasing mobile phase conductivity (1–25 mS/cm). However at pH 4 on SP Sepharose XL, Fab dynamic binding capacity increased from 130 to 160 (mg/mL media) as mobile phase conductivity changed from 1 to 5 mS/cm. Decreasing protein net charge by increasing pH from 4 to 5 at 1.3 mS/cm caused dynamic binding capacity to increase from 130 to 180 mg/mL. Confocal scanning laser microscopy studies indicate such increases were due to faster intra-particle mass transport and hence greater utilization of the media's available binding capacity. Such results are in agreement with recent studies related to ion exchange of whole antibody molecules under similar conditions.

Biotechnol. Bioeng. 2007;96: 515–524.

KEYWORDS: antibody fragment; Fab; ion exchange chromatography; confocal microscopy

Introduction

There has been growing interest in therapeutic and other uses of antibodies and antibody fragments. Currently there are over 13 medically approved monoclonal antibodies (MAbs), and 75 MAbs under evaluation in clinical trials (Coco-Martin, 2004). Truncated forms of antibodies, especially those possessing binding function including Fabs or Fab′2s and single chain Fv forms, have also been used for a variety of clinical applications. Antibody fragments can be an interesting choice for applications where Fc-mediated effector functions are not beneficial. They exhibit a shorter circulating half-life than full length antibodies, but their smaller size can be an advantage in applications such as tumor penetration and for medical imaging (Anderssen and Reilly, 2004; Roque et al., 2004).

Many purification strategies for antibodies and their fragments have been developed based on different adsorption-desorption principles. At present the most widely used technique to capture MAbs is affinity chromatography on immobilized protein A sorbents (Brorson et al., 2003; Fahrner et al., 1999a,b, 2001; Hahn et al., 2003, 2005, 2006; Ishihara et al., 2005; McCue et al., 2003) followed by ion exchange chromatography (Fahrner et al., 1999). For the purification of Fab fragments several different techniques like Protein L affinity-, immobilized metal affinity-, ion exchange-, hydroxyapatite-, hydrophobic interaction-, hydrophobic charge induction-, and size exclusion chromatography have been employed (Roque and Lowe, 2005; Willems et al., 2003; Wlad et al., 2001).

The adsorption of proteins onto different chromatographic matrices has been studied extensively. Most of these studies have been carried out as batch or column experiments in which the adsorbent is considered as a bulk phase. Recently, confocal scanning laser microscopy has been introduced as an alternative and complementary method for studying protein adsorption at the matrix level (Dziennik et al., 2003; Hubbuch et al., 2003a,b; Linden et al., 1999, 2002; Ljunglöf and Hjorth, 1996; Ljunglöf and Thömmes, 1998; Ljunglöf et al., 1999; Subramanian and Hommerding, 2005; Zhou et al., 2006). With this technique it is possible to study intra-particle protein and DNA concentrations, and also ligand distributions, directly within individual adsorbent particles (Larsson et al., 2002, 2003;

Correspondence to: A. Ljunglöf

Ljunglöf et al., 2000). The high optical resolution (e.g., <1 μm) obtained with confocal microscopy allows visualization of the adsorption process after labeling of the protein molecules with a fluorescent probe. Confocal measurements following single component adsorption to individual ion exchange adsorbent particles have revealed a very interesting phenomenon. Under certain conditions of ionic strength and pH, temporary concentration overshoots, that is, adsorbed phase concentrations that are higher at certain radial positions within the particle compared with positions closer to the particle surface or to the center, have been observed during the adsorption process (Dziennik et al., 2003; Hubbuch et al., 2002, 2003a,b; Linden, 2001; Ljunglöf, 2002; Ljunglöf and Thömmes, 1998). To address the possibility that the observed concentration overshoots are related to labeling of the protein with fluorescent probes, investigations have been performed with unlabeled proteins using an UV-laser source or multiphoton excitation (Dziennik et al., 2003; Lenhoff and Dziennik, 1999). The results confirmed that the concentration overshoots are formed in the absence of fluorescence labeling. Theoretical models explaining the phenomena have recently been proposed (Dziennik et al., 2003; Grimes, 2002; Grimes and Liapis, 2002; Liapis and Grimes, 2005; Liapis et al., 2001; Zhang et al., 2004a,b).

The authors have earlier reported experimental studies on cation exchange of different MAbs (Harinarayan et al., 2002, 2006; Ljunglöf et al., 2003). The effect of pH and conductivity on the adsorption to two different commercial cation exchange media sulfopropyl (SP Sepharose Fast Flow and SP Sepharose XL) was investigated. The dynamic binding capacity of MAbs was shown to be significantly reduced at low conductivities and low pH (high net protein charge). Confocal scanning laser microscopy indicated that under the conditions studied proteins are unable to penetrate deeply into porous chromatography beads. Confocal microscopy shows the possibility that protein molecules adsorbed at pore channels near the external surface of the media hinder other molecules from entering the pores and that such exclusion is reduced at high conductivity, leading to a direct relationship between net protein charge and the solution conductivity yielding optimal dynamic capacity (Harinarayan et al., 2006).

The aim of the present work was to investigate how the binding capacity and mass transport of Fab fragments are influenced by ionic strength and pH, and if Fabs show similar exclusion effects as MAbs. Confocal microscopy was used to study protein adsorption at the bead level, and the results were compared with measurements of dynamic capacity in packed beds.

Materials and Methods

Instrumentation

Chromatography experiments were performed on an ÄKTAexplorer^{TM} 100 (GE Healthcare, Uppsala, Sweden). Control experiments comparing retention volumes of labeled and unlabeled Fab fragments were performed on an ÄKTAexplorer 10 (GE Healthcare). Confocal microscopy measurements were made with a Leica TCS SP confocal scanning laser microscope equipped with a He/Ne laser and with TCS NT software for image evaluation. A UV laser source was used for excitation of intrinsic fluorescence from non-labeled proteins, and the emitted fluorescence was detected with a Leica DC 300 CCD camera. Fluorescence emission in the fluid phase from finite bath experiments was measured with a SPEX Fluorolog-3 fluorescence spectrometer purchased from JY Horiba (Edison, NJ).

Adsorbents, Proteins, and Chemicals

Cation exchange resins of similar ligand density and ion exchange capacity, SP Sepharose XL (200 μmol H^+/mL) and SP Sepharose Fast Flow (200 μmol H^+/mL), and Cy5 reactive dye were obtained from GE Healthcare. Antigen-binding fragment (Fab), with an isoelectric point of 8.1, was from Genentech Inc.'s (South San Francisco, CA). Net charge versus pH for the Fab-fragment (based on the amino acid sequence) is given in Figure 1. Protein labeling with Cy5 was performed according to the standard procedure recommended by the manufacturer. To avoid light attenuation due to reabsorption or inner filtering (Ljunglöf, 2002; Van Oostvelt and Bauwens, 1990), the labeled protein was mixed with unlabeled protein in a ratio of 1:20. Buffers utilized were 15 mM Sodium acetate (Fisher Scientific, Hampton, NH) for pH 4 and 5 that was pH adjusted with glacial acetic acid (Mallinckrodt, Phillipsburg, NJ). Proteins (8 mg/mL) were diafiltered into the two different buffers. A stock solution of 5 M NaCl was added to obtain conductivities of 1.25, 5, 10, 15, and 25 mS/cm. Elution buffer was made up with 20 mM MES (2-morpholinoethanesulfonic acid, Sigma, St. Louis, MO) 4.5 mM Sodium MES, 1.5 M NaCl, pH 5.5.

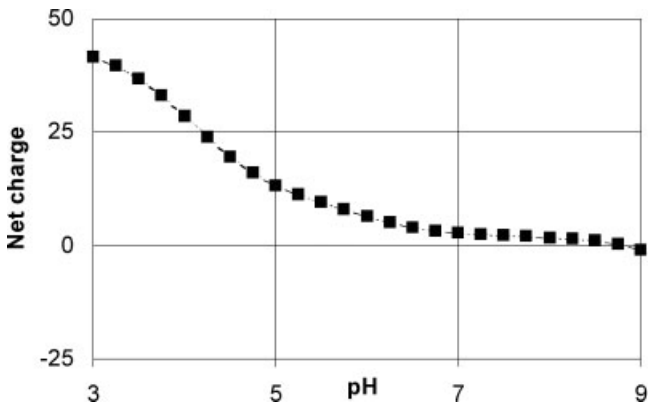

Figure 1. Net charge for Fab based on amino acid sequence as a function of pH. Reprinted by permission of Genentech Inc. and General Electric Company.

DOI 10.1002/bit

Adsorption Isotherms

Equilibrium data at various pH and buffer concentrations were obtained using a static micro batch method developed at GE Healthcare (Linden et al., 1999; Ljunglöf et al., 2000). The equilibrium data obtained were described using a Langmuir isotherm with the association equilibrium constant K_a and the maximum capacity Q_{max} as parameters (Eq. 1).

$$Q_{eq} = Q_{max} \cdot \frac{K_a \cdot c_{eq}}{1 + K_a \cdot c_{eq}} \quad (1)$$

Measurement of Dynamic Binding Capacity

Dynamic binding capacities for the Fab was obtained at pH 4 and 5 with conductivities of 1, 5, 10, 15, and 25 mS/cm on SP Sepharose XL and SP Sepharose Fast Flow resins in Omnifit™ columns (VWR) diameter of 0.66 cm and bed height of 10 cm. The resins were equilibrated using three column volumes (CV) of the load buffer. All chromatography experiments were performed at a flow velocity of 100 cm/h. The resins were regenerated and stored using 0.5 N NaOH and 0.1 N NaOH, respectively. The protein was loaded onto the resin to 10% breakthrough capacity ($Q_{B,\ 10\%}$) based on the protein load absorbance (A_{280}). Unbound proteins were then washed away using 5 CV of the same buffer. Elution was performed by a linear gradient of 6 CV using the equilibration buffer and elution buffer (20 mM MES, 4.5 mM Sodium MES, 1.5 M NaCl, pH 5.5), followed by 6 CV with elution buffer. Dynamic binding capacities were obtained according to Eq. (2).

$$Q_{B,\ 10\%} = \frac{(V_{10\%} - V_0) * C_0}{V_c} \quad (2)$$

where $V_{10\%}$ = volume of protein loaded at 10% breakthrough, C_0 = sample concentration (mg/mL) and V_c = geogeometric total volume and V_0 = void volume. Three replicate experiments were performed for each condition. Averages of the triplicate capacities are reported (Table I).

Table I. Least square estimates of parameters in the Langmuir isotherm model.

Conditions			
pH	mS/cm	Q_{max} mg/mL$_{bed}$	K_{ads} mL/mg[a]
4	1.3	295 ± n.d.	169 ± n.d.
4	5	173 ± 3	24 ± 3
4	10	158 ± 3	53 ± 9
4	15	146 ± 4	12 ± 1
5	1.3	242 ± 11	109 ± 27
5	5	119 ± 4	5 ± 1
5	10	52 ± 18	0.2 ± 0

n.d., not determined.
[a]Assuming interstitial porosity of 0.32.

Confocal Microscopy

Twenty microliters protein solution (i.e., ~8 mg/mL in various buffers) was filled in a reaction vessel equipped with a hanging stirrer. The reaction vessel was connected to a MultiTemp™ II water bath (GE Healthcare), and the temperature was set to 21°C. The adsorption experiment was started by adding a defined amount of gel slurry, that is, settled gel diluted 1:2 (v/v) with buffer, to the stirred protein solution. Samples were then taken from the reaction vessel at fixed times, and individual adsorbent particles were immediately analyzed by acquisition of two-dimensional confocal images perpendicular to the optical axis (i.e., xy-scan) (Ljunglöf and Hjorth, 1996; Ljunglöf and Thömmes, 1998). A 63 × 1.2 water immersion objective was used for all measurements. The laser provided excitation of Cy5 at 633 nm, and emitted fluorescent light was detected between 643 and 800 nm. To reduce background fluorescence and noise, the images were generated by accumulating four scans per image. The image size was 512 × 512 pixels and the pixel size was 0.31 μm.

The distribution of fluorescent molecules across the adsorbent particles was obtained by translating the confocal images into fluorescence intensity profiles. The overall fluorescence within the particles and the relative solid phase concentration (Q_{rel}) was calculated as previously described (Ljunglöf and Thömmes, 1998). By subsequently relating the relative fluorescence intensity obtained at different times to the value at equilibrium (Q_{rel}^{∞}), the degree of saturation versus time (F) could be calculated according to Eq. (3).

$$F = \frac{Q_{rel}}{Q_{rel}^{\infty}} \quad (3)$$

The results obtained by direct measurement using confocal microscopy were also compared with the indirect measurement obtained via the fluid phase concentration as earlier described (Ljunglöf and Thömmes, 1998). A good agreement was obtained between the uptake profiles. The results confirm correct calibration of the confocal microscope and that confocal measurement in individual adsorbent particle gives a realistic picture of the kinetics of protein uptake (data not shown).

Elution Studies in a Linear Gradient to Compare Retention of Labeled and Unlabeled Fab

In order to investigate the influence of protein labeling, experiments to compare the retention factor and conductivity during elution from SP Sepharose XL were performed employing ÄKTAexplorer 10. Twenty-five microliters samples of unlabelled protein and protein-Cy5 conjugate in 50 mM acetate buffer pH 4.0 were loaded onto a SP Sepharose XL column (5 mm × 10.4 cm; 1 column volume 8.2 mL) with a linear flow velocity of 50 cm/h (0.65 mL/min). After sample load a linear salt gradient from 0 to 0.55 M NaCl in 50 mM acetate buffer was used

to elute the bound protein. The elution was monitored by detecting the absorbance at 280 and 650 nm and conductivity (mS/cm). Retention volume (V_r) and elution conductivity were derived from the eluted peak maxima, and the retention factor k' was calculated according to Eq. (4), using retention volume for acetone, V_0, as the accessible volume.

$$k' = \frac{V_r - V_0}{V_0} \quad (4)$$

Control Experiment With Unlabeled Proteins

To exclude the possibility that the labeling of the proteins with fluorescent probes (i.e., Cy5) could introduce experimental artefacts, control experiments were performed by excitation and detection of intrinsic fluorescence arising directly from amino acid residues in the unlabeled protein molecules (Lakowicz, 1999). Batch incubation was performed in a reaction tube by end-over-end rotation. Samples were removed from the reaction tube at defined times. Excitation of intrinsic fluorescence was then performed using a UV source (340–380 nm), and emitted fluorescent light was immediately detected by a CCD camera (in non-confocal mode) at wavelength above 420 nm. Continued irradiation of the sample with UV-light ($\geq$1 s) resulted in strong fading of the fluorescent signal.

Results and Discussion

Adsorption Isotherms

Adsorption isotherms of the Fab on SP Sepharose XL were measured at pH 4 and 5 at conductivities between 1 and 15 mS/cm. The results obtained are shown in Figure 2. In order to quantify the effect of pH and ionic strength on the adsorption equilibrium, parameters in the Langmuir adsorption isotherm model were obtained by fitting Eq. (1) to the data shown in Figure 2. The least square estimates of model parameters are given in Table I.

The results showed that while at pH 5 the effect of ionic strength seems to follow the typical ion exchange behavior described by a decrease in maximum adsorption capacity (Q_{max}) and association constant (K_a) with an increase in ionic strength (Table I), at pH 4 a more complex situation can be observed. At this pH a very weak decrease in capacity was observed when conductivity increased from 5 to 15 mS/cm. Furthermore, association constant values appear to show a maximum in this conductivity range with a local minimum in association constant seen at 5 mS/cm (Table I). This minimum could indicate that a weaker interaction between Fab and a resin binding site was occurring. Such interaction could then translate into a different rate of mass transport inside the pores of adsorbent particle, which could manifest itself in higher binding capacities under the dynamic conditions as in typical column experiments.

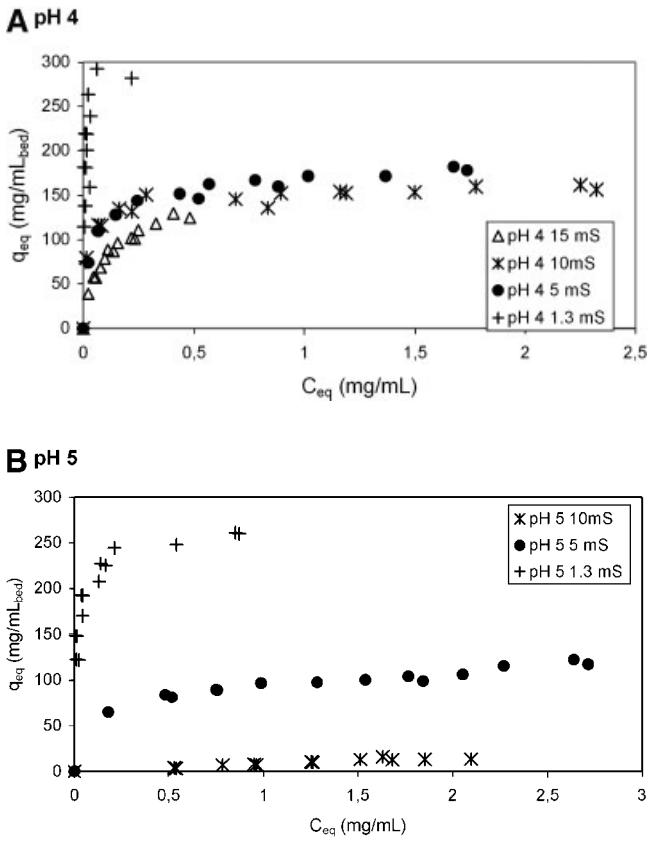

Figure 2. Adsorption isotherms of Fab adsorbing to SP Sepharose XL. **A**: pH 4, conductivity 1.3–15 mS/cm, (**B**) pH 5, conductivity 1.3–10 mS/cm. Reprinted by permission of Genentech Inc. and General Electric Company.

Influence of pH and Conductivity on Dynamic Binding Capacity

Dynamic binding capacity on SP Sepharose XL and SP Sepharose Fast Flow was measured at pH 4 and 5 with conductivities between 1 and 25 mS/cm (Table II, Fig. 3). On SP Sepharose XL, pH 5 and SP Sepharose Fast Flow pH 4 and 5, the dynamic binding capacity (DBC at 10% breakthrough) decreases at increased conductivity. The decrease in capacity at higher conductivity is expected and is well characterized (Brooks and Cramer, 1992). However, on SP Sepharose XL, pH 4, the dynamic capacity increases, from 130 to 160 mg/mL (i.e., 23%), when increasing the conductivity from 1.3 to 5 mS/cm, while further increase in conductivity results in decreased capacity. Furthermore, by increasing pH from 4 to 5 at 1.3 mS/cm the dynamic capacity increases from 130 to 180 mg/mL (i.e., 38%).

As can be seen from the batch uptake curves derived from the confocal microscopy measurements (Fig. 5a), the intra-particle mass transport at pH 4, 1.3 mS/cm, is relatively slow.

DOI 10.1002/bit

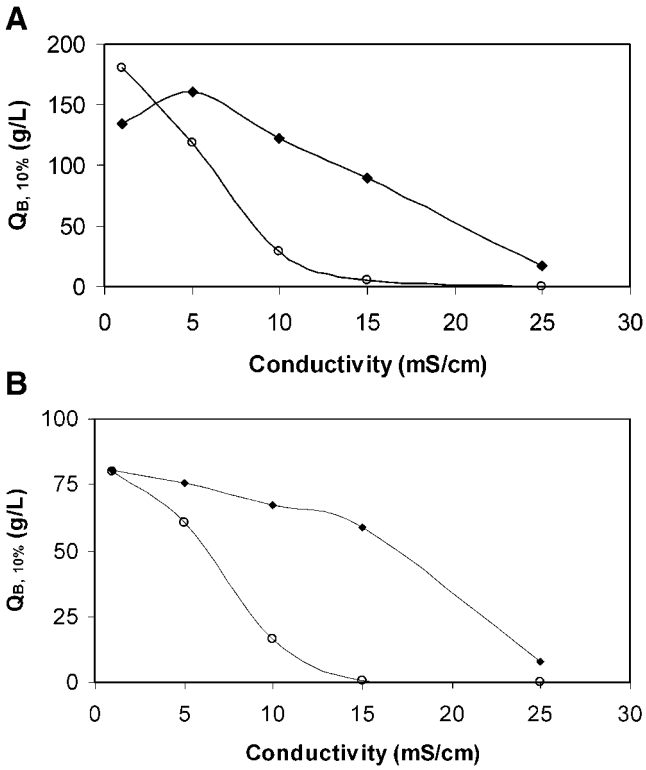

Figure 3. Dynamic capacity for Fab at pH 4 (◆) and pH 5 (○). **A**: SP Sepharose XL, (**B**) SP Sepharose Fast Flow. Reprinted by permission of Genentech Inc. and General Electric Company.

Thus, approximately 20% saturation is obtained after 5 min, and 50% after 10 min incubation time. The corresponding values at 5 mS/cm are 60 and 80%, respectively. Thus even if the equilibrium capacity decreases at increased conductivity, the faster intra-particle mass transport results in higher utilization of the available binding capacity (Fig. 4) resulting in increased dynamic capacity (Table II).

One reason for the slow intra-particle mass transport at pH 4, 1.3 mS/cm, may be explained by reduced transport

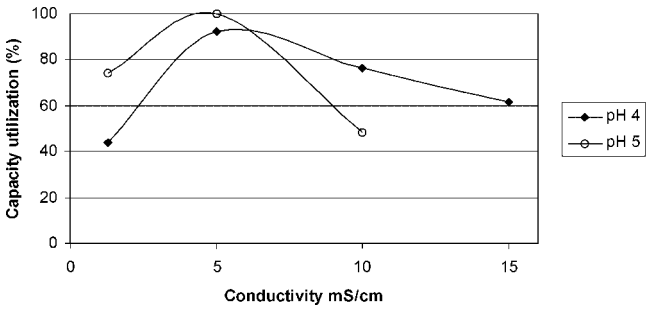

Figure 4. Capacity utilization of SP Sepharose XL at varying pH and conductivity. Reprinted by permission of Genentech Inc. and General Electric Company.

Table II. Binding capacity for SP Sepharose XL at varying pH and conductivity.

pH	Conductivity (mS/cm)	Q_B (mg/mL)	Q_B/Q_{eq} (%)
4	1.3	130	44
4	5	160	93
4	10	120	76
4	15	90	62
4	25	0	—
5	1.3	180	74
5	5	120	100
5	10	25	48
5	15	0	—

effects as reported earlier for MAbs and SP Sepharose XL (Harinarayan et al., 2006). Such reduced transport appeared to be due to adsorbed charged proteins inhibiting the pore transport of similarly charged proteins. In the present study protein transport increased with pH (an increase in pH from 4 to 5 results in a decrease of 16 positive charges, Fig. 1) or conductivity (increased charge shielding), resulting in increased dynamic binding capacity. In contrast to SP Sepharose XL, no equivalent effect can be observed under these conditions on SP Sepharose Fast Flow. Both adsorbents are based on porous 6% cross-linked agarose (average diameter 9×10^{-5} m), and have the same ionic capacity. However, whereas SP Sepharose Fast Flow is characterized by a relatively open pore network with sulfopropyl (SP) groups attached to the pore walls, dextran has been grafted to the agarose backbone before coupling of the ligands to Sepharose XL. This procedure basically fills the pores of the agarose particles with ligand carrying flexible polymer chains, and increases the effective interaction volume and results in higher protein binding capacity (Staby and Holm Jensen, 2001; Staby et al., 1998; Staby et al., 2004; Thömmes, 1999). As a consequence, proteins interacting with SP ligands on the dextran chains may be more able to influence the pore transport of other proteins.

Furthermore, NMR studies have shown that the random movement of charged dextran polymers increase with conductivity. An increase in the flexibility of such ion exchange groups tethering polymers might favor both increased protein transport (through the dextran layer) and more favorable protein-ligand interactions resulting in greater equilibrium capacity (Herbert Bauman, GE Healthcare, personal communication; Harinarayan et al., 2006).

Adsorption Patterns

Confocal microscopic analyses of SP Sepharose XL particles at different times during the finite bath uptake, results in confocal images representing the adsorption progress within individual adsorbent particles. Thus, the images show how the protein molecules penetrate the particles from the outer rim to the center of the particles until they are completely and evenly saturated. Figure 5 shows series of confocal

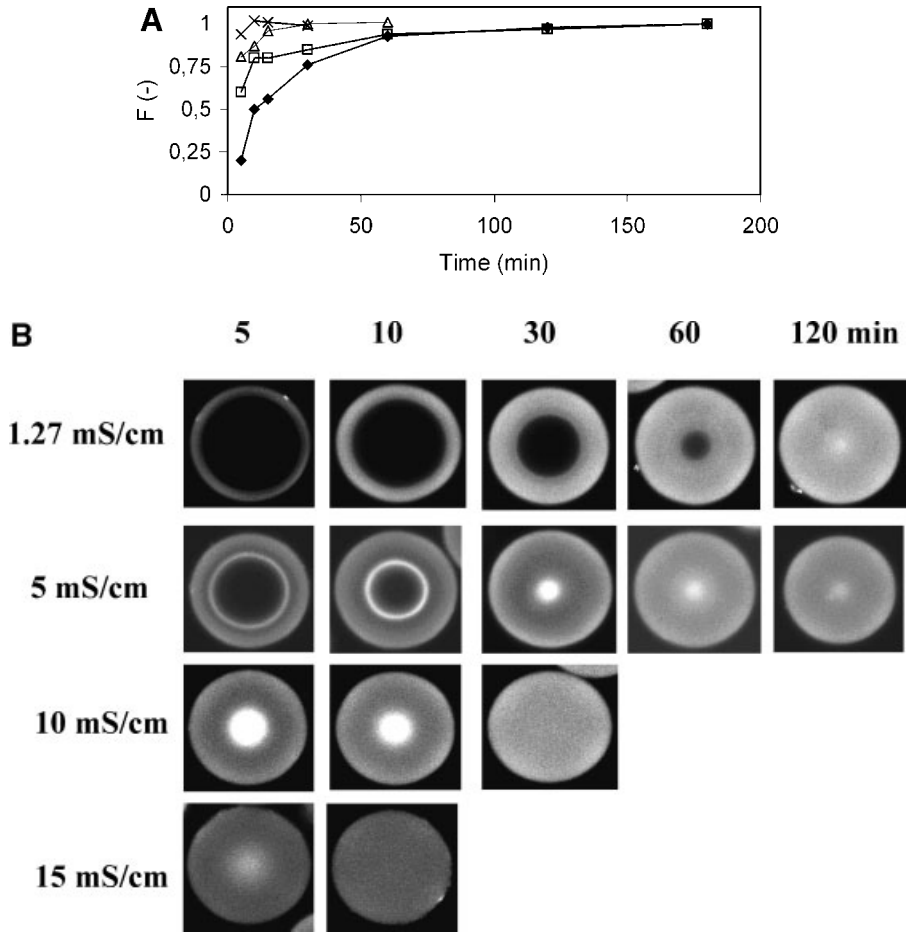

Figure 5. **a**: Uptake curves to SP Sepharose XL, pH 4.0. Conductivity: diamonds 1.2, squares 5, triangles 10, and cross 15 mS/cm. Reprinted by permission of Genentech Inc. and General Electric Company. **b**: Confocal images obtained at different times during batch adsorption of Fab to SP Sepharose XL at pH 4, conductivity varied between 1.27 and 15 mS/cm. Reprinted by permission of Genentech Inc. and General Electric Company.

images, and corresponding uptake curves, for the adsorption of Fab at pH 4. At low conductivity (1.3 mS/cm) sharp adsorption fronts are obtained and the particles are saturated after approximately 2 h incubation. However at increased conductivity (5 mS/cm) a quite different adsorption pattern can be observed. Thus the fluorescent signal reveals that a concentration "overshoot" or "ring" is seen to form early during the adsorption process. With time the overshoot moves towards the center of the particle, and finally at equilibrium it disappears. Therefore this intraparticle transport phenomenon can be described as a temporary "concentration overshoot" as earlier introduced (Dziennik et al., 2003; Grimes, 2002; Grimes and Liapis, 2002; Liapis and Grimes, 2005; Liapis et al., 2001; Linden, 2001, Ljunglöf, 2002; Zhang et al., 2005a). At 10 mS/cm the mass transport is much faster, saturation is obtained after 30 min, and again a temporary concentration overshoot can be observed. At 15 mS/cm the mass transport is even faster and saturation is obtained already after ~10 min. A temporary overshoot can be observed, however, the magnitude of the overshoot is much lower. Finally at 25 mS/cm no protein adsorption can be observed (i.e., no binding capacity). At pH 5, a temporary overshoot can be observed at 1.3 mS/cm (Fig. 6). Increased conductivity results in faster saturation of the adsorbent particles and no overshoot phenomenon can be observed.

Recently it was reported that a concentration overshoot occurs when two proteins (i.e., lysozyme and cytochrome c) are competitively adsorbed to SP Sepharose Fast Flow (Martin et al., 2005). Furthermore, the effect on fluorescence labeling on lysozyme adsorption to SP Sepharose Fast Flow has been investigated (Teske et al., 2005). It was reported that the retention time of lysozyme-dye conjugates differ significantly from unlabeled lysozyme. The result suggested that the concentration overshoot could be caused by displacement of weaker binding labeled lysozyme by stronger binding unlabeled lysozyme. To exclude the possibility that observed concentration overshoots for Fab fragments are artefacts related to the fluorescence labeling, two different control experiments were performed. In the first experiment a comparison of retention (retention factor and conductivity) obtained with labeled and unlabeled Fab

DOI 10.1002/bit

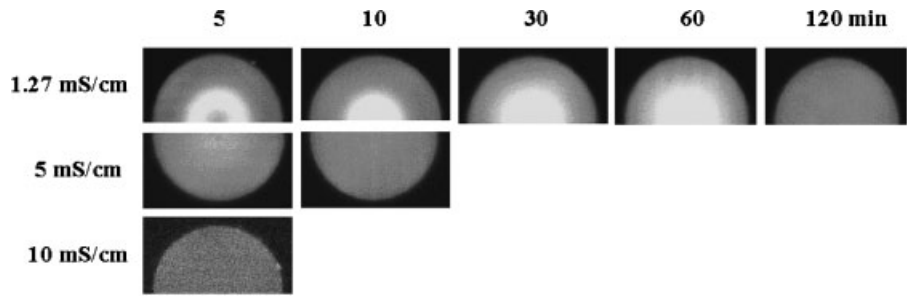

Figure 6. Confocal images obtained at different times during batch adsorption of Fab to SP Sepharose XL at pH 5, conductivity varied between 1.27 and 10 mS/cm. Reprinted by permission of Genentech Inc. and General Electric Company.

fragments was performed by gradient elution from SP Sepharose XL. The result indicates that labeled Fab fragment binds only somewhat weaker to the cation exchanger than unlabeled protein (Fig. 7; Table III). The second control experiment was carried out by measurement of intrinsic fluorescence originating from unlabeled protein molecules, by use of a UV light source and a CCD camera. Microscopy images, obtained during Fab uptake at pH 4, conductivity 5 mS/cm, are shown in Figure 8. As can be seen concentration overshoots can be observed also during adsorption of unlabeled protein, and the dynamics of their formation are in accordance with the corresponding results obtained with fluorescent labeled protein observed with confocal microscopy (Fig. 5). Thus, in this case it could be concluded the observed concentration overshoots are not artefacts mainly caused by the fluorescence labeling. This result is in accordance with previous studies by Dziennik et al. (2003) who observed the occurrence of concentration overshoots,

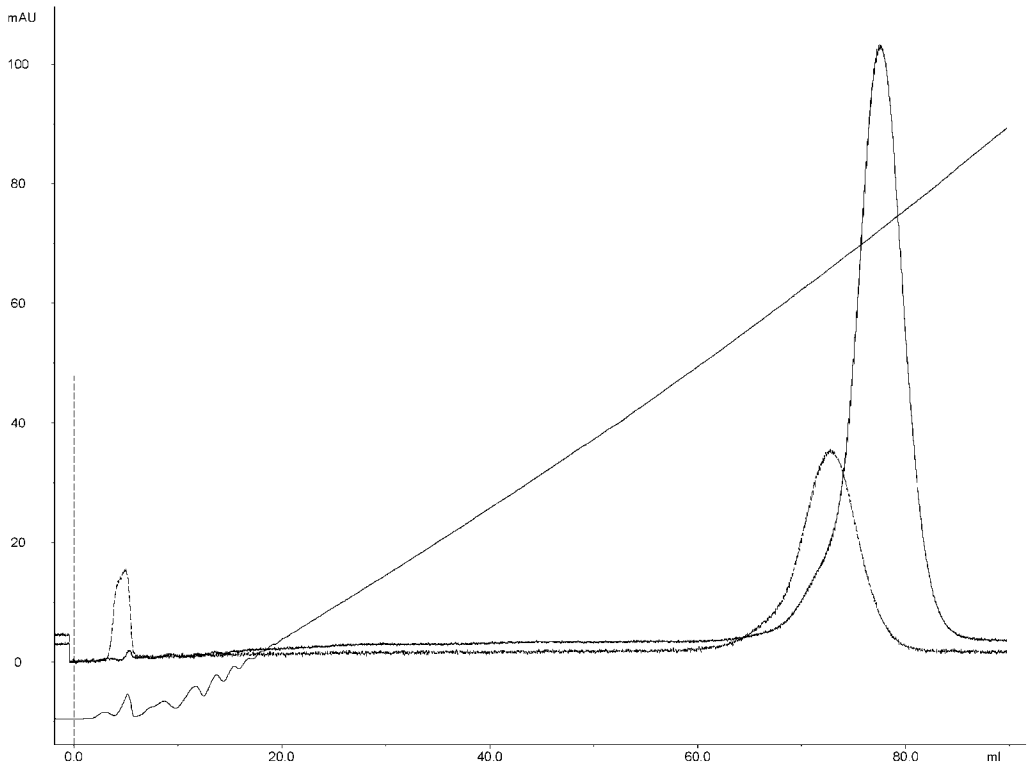

Figure 7. Gradient elution from SP Sepharose XL. Sample: Fab labelled with Cy5. Gradient elution: 50 mM acetate pH 4, 0–0.55 M NaCl; 11 column volumes. Linear velocity 50 cm/h (residence time 12.5 min). Unlabeled Fab detected at 280 nm (continuous line) and labeled Fab at 650 (broken line). Reprinted by permission of Genentech Inc. and General Electric Company.

Table III. Retention factor and conductivity obtained for labeled and unlabeled Fab.

Sample	k'	Cond. (mS/cm)
Fab unlabeled (280 nm)	8.56	27.3
Fab unlabeled (650 nm)	—	—
Fab Cy5 (280 nm)	8.56	27.3
Fab Cy5 (650 nm)	7.98	25.3

for adsorption of unlabeled lysozyme to SP Sepharose Fast Flow, using an UV-laser source and by multi-photon excitation (Lenhoff and Dziennik, 1999). In that study it was also shown that the concentration overshoot phenomenon is at least qualitatively independent on the labeling with fluorescent tracers. Similar results have also been observed in our laboratories with unlabeled MAbs (data not shown). Considering the somewhat weaker binding of labeled Fab fragment, a contribution to the overshoot phenomenon by displacement of labeled protein by unlabeled can not be entirely excluded. However present experiments with unlabeled sample show that displacement is not the main contributor to the overshoot phenomenon we have noticed and earlier reported.

Summary and Conclusions

The aim of the work was to investigate how the binding capacity and mass transport of Fab is influenced by ionic strength and pH (protein charge). Confocal microscopy was used to study protein adsorption at the bead level, adsorption isotherms were determined, and the results were compared with measurements of dynamic capacity in packed beds.

The column experiments showed that:

— Protein exclusion on SP Sepharose XL occurred at low pH (high protein charge) and low conductivity, while no such effect could be observed under these conditions on SP Sepharose Fast Flow.
— Increased dynamic capacity could be obtained either by increasing pH (decrease protein charge) or conductivity (i.e., ionic strength) of the solution environment.

Confocal microscopy analysis of individual adsorbent particles revealed that:

— Increased pH and conductivity speeded up intra-particle mass transport.
— Intra-particle concentration overshoots were formed at certain combinations of pH and conductivity.

In regard to mechanistic description of these phenomena the most important observations in the present work are that:

— Adsorbed phase concentrations could be observed that were higher at certain radial positions within the particle compared with positions closer to the particle surface or to the center.
— The occurrence and magnitude of concentration overshoots was strongly influenced both by pH (i.e., protein net charge) and conductivity (i.e., ionic strength).
— The concentration overshoots appeared to be suppressed by increasing pH and conductivity.
— The transient increase in concentration within the particle relative to the particle rim implied that protein molecules were transported against a concentration gradient.
— The protein concentration within the accumulation zone (overshoot) leveled off while the system moved towards equilibrium. This suggests that the capacity was increased within the adsorption front during a transition state.

These observations indicate that phenomena involving electrophoretic transport of charged species and dynamic variation of the electrostatic interactions occurring between charged molecules and charged surfaces in the pores of ion exchange resins contribute to the formation, relative magnitude, and speed of propagation of the concentration overshoot. A recent review paper (Liapis and Grimes, 2005) discuss these phenomena from the mechanistic modeling perspective.

While providing practical insight to factors affecting the purification of a significant family of biopharmaceutical

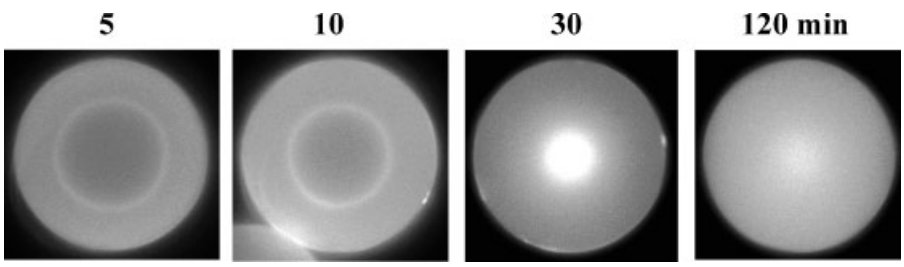

Figure 8. Microscopy images obtained at different times during batch adsorption. of unlabeled Fab to SP Sepharose XL. Buffer: Acetate pH 4, 5 mS/cm. Reprinted by permission of Genentech Inc. and General Electric Company.

DOI 10.1002/bit

products, the present work also highlights emerging consensus that protein purification by ion exchange chromatography involves complex electro-physico-chemical phenomena occurring at the microscopic (molecular) level. From theses perspective, the recent works by Zhang et al. (2004a,b, 2005a,b) are powerful examples of the use of molecular dynamic simulations in the studies of ion exchange systems, and how such studies could be employed in a multi-scale modeling and simulations to fully utilize the separation potential of the current and a better design of future chromatography resins.

References

Anderssen DC, Reilly DE. 2004. Production technologies for monoclonal antibodies and their fragments. Curr Opin Biotechnol 15:456–462.

Brooks CA, Cramer S. 1992. Steric mass-action ion exchange: Displacements profiles and induced salt gradients. AIChE J 38(12):1969–1978.

Brorson K, Brown J, Hamilton E, Stein KE. 2003. Identification of proteina A media performance attributes that can be monitored as surrogates for retrovirus clearance during extended re-use. J Chromatogr A 989:155–163.

Coco-Martin JM. 2004. Mammalian expression of therapeutic proteins. Bio Process Int 2:32–40.

Dziennik SR, Belcher EB, Barker GA, DeBergalis MJ, Fernandez SE, Lenhoff AM. 2003. Nondiffusive mechanisms enhance protein uptake rates inion exchange particles. PNAS 100(2):420–425.

Fahrner RL, Whitney DH, Vanderlaan M, Blank GS. 1999a. Performance comparison of protein A affinity-chromatography sorbents for purifying recombinant monoclonal antibodies. Biotechnol Appl Biochem 30(2):121–128.

Fahrner RL, Blank G, Zapata GA. 1999b. Expanded bed protein A affinity chromatography of recombinant humanized monoclonal antibody: Process development, operation, and comparison with packed bed method. J Biotechnol 75(2–3):273–280.

Fahrner RL, Knudsen HL, Basey CD, Galan W, Feuerhelm D, Vanderlaan M, Blank G. 2001. Industrial purification of pharmaceutical antibodies: Development, operation and validation of chromatography processes. Biotechnol Genetic Rev 18:301–327.

Grimes BA, Ph. D. 2002. Dissertion, Department of Chemical Engineering, University of Missouri-Rolla, Missouri, USA.

Grimes BA, Liapis AI. 2002. The interplay of diffusional and electrophoretic transport mechanisms of charged solutes in the liquid film surrounding charged nonporous adsorbent particles employed in finite bath adsorption systems. J Colloid Interface Sci 248(2):504–520.

Hahn R, Schegel R, Jungbauer A. 2003. Comparison of protein A affinity sorbents. J Chromatogr B 790:35–51.

Hahn R, Bauerhansl P, Shimahra K, Wizniewski C, Tscheliessnig A, Jungbauer A. 2005. Comparison of protein A affinity sorbents II: Mass transfer properties. J Chromatogr A 1093:98–110.

Hahn R, Shimahara K, Steindl F, Jungbauer J. 2006. Comparison of protein A affinity sorbents III: Life time study. J Chromatogr A 1102:224–231.

Harinarayan C, Mueller J, Ljunglöf A, Fahrner R, van Reis R. 2002. Development of novel ion exchange process conditions in antibody purification. Presentation at Antibody Production and Downstream Processing, IBC conference, San Diego, USA, November 2002.

Harinarayan C, Mueller J, Ljunglöf A, Fahrner R, van Alstine J, van Reis R. 2006. An exclusion mechanism in ion exchange chromatography. Biotechnol Bioeng 95:775–787.

Hubbuch J, Linden T, Knieps E, Thömmes J, Kula M-R. 2002. Dynamics of protein uptake within the adsorbent particle during packed bed chromatography. Biotechnol Bioeng 80(4):359–368.

Hubbuch J, Linden T, Knieps E, Ljunglőf A, Thommes J, Kula MR. 2003a. Mechanisms in kinetics of transport in chromatography media studied by confocal laser scanning microscopy. Part I. The interplay of sorbent structure and fluid phase conditions. J Chromatogr A 1021: 93–104.

Hubbuch J, Linden T, Knieps E, Thommes J, Kula MR. 2003b. Mechanisms in kinetics of transport in chromatography media studied by confocal laser scanning microscopy. Part II. Impact on chromatographic separations. J Chromatogr A 1021:105–115.

Ishihara T, Kadoya T, Yoshida H, Tamada T, Yamamoto S. 2005. Rational methods for predicting human monoclonal antibodies retention in protein A affinity chromatography and cation exchange chromatography Structure-based chromatography design for monoclonal antibodies. J Chromatogr A 1093:126–138.

Lakowicz JR. 1999. Principles of fluorescence spectroscopy. New York: Kluwer Academic/Plenum Publishers, Chapter 16.

Larsson M, Ljunglöf A, Knuuttila K-G, Lindgren J. 2002. Raman and fluorescence spectroscopy applied to polymeric chromatographic adsorbent particles. J Chromatogr A 954:151–158.

Larsson M, Lindgren J, Ljunglöf A, Knuuttila K-G. 2003. Ligand distributions in agarose particles as determined by confocal Raman spectroscopy and confocal scanning laser microscopy. Appl Spectrosc 57(3): 251–255.

Lenhoff AM, Dziennik SR. 1999. Use of confocal microscopy to resolve protein transport mechanisms in chromatographic particles. Annual meeting of the American institute of chemical engineers. Paper 22b. Dallas, USA.

Liapis AI. Grimes BA. 2005. The coupling of the electrostatic potential with the transport and adsorption mechanism in ionexchange chromatography systems: Theory and experiments. J Sep Sci 28:1909–1926.

Liapis AI, Grimes BA, Lacki K, Neretnieks I. 2001. Modeling and analysis of the dynamic behavior of mechanisms that result in the development of inner radial humps in the concentration of a single adsorbate in the adsorbed phase of porous particles observed in confocal scanning laser microscopy experiments: Diffusional mass transfer and adsorption in the presence of an electrical double layer. J Chromatogr A 921(2):135–145.

Linden T. 2001. Doctoral thesis: ''Untersuchungen zum inneren Transport bei der Proteinadsorption an poröse Medien mittels konfokaler Laser-Raster-Mikroskopie''. Heinrich-Heine-Universität Duesseldorf, Germany.

Linden T, Ljunglöf A, Kula M-R, Thömmes J. 1999. Visualizing two-component protein diffusion in porous adsorbents by confocal scanning laser microscopy. Biotechnol Bioeng 65(6):622–630.

Linden T, Ljunglöf A, Hagel L, Kula M-R, Thömmes J. 2002. Visualizing patterns of protein uptake to porous media using confocal scanning laser microscopy. Sep Sci Tech 37(1):1–32.

Ljunglöf A. 2002. Doctoral thesis: ''Direct observation of biomolecule adsorption and spatial distribution of functional groups in chromatographic adsorbent particles''. Uppsala University, Sweden. www.uu.se/avhandlingar.

Ljunglöf A, Hjorth R. 1996. Confocal microscopy as a tool for studying protein adsorption to chromatographic matrices. J Chromatogr A 743: 75–83.

Ljunglöf A, Thömmes J. 1998. Visualizing intraparticle protein transport in porous adsorbents by confocal microscopy. J Chromatogr 813:387–395.

Ljunglöf A, Bergvall P, Bhikhabhai R, Hjorth R. 1999. Direct visualization of plasmid DNA in individual chromatography adsorbent particles by confocal scanning laser microscopy. J Chromatogr A 844:129–135.

Ljunglöf A, Larsson M, Knuuttila K-G, Lindgren J. 2000. Measurement of ligand distribution in individual adsorbent particles using confocal scanning laser microscopy and confocal micro-Raman spectroscopy. J Chromatogr A 893:235–244.

Ljunglöf A, Kjellgren A, Harinarayan C, Mueller J, Fahrner R, van Reis R. 2003. Adsorption oif monoclonal antibodies to cation exchange chromatography media. A study with confocal microscopy. Presentation at Prep 2003, Washington DC, June 2003.

Martin C, Iberer G, Ubiera A, Carta G. 2005. Two-component protein adsorption kinetics in porous ion exchange media. J Chromatogr A 1079(1–2):105–115.

McCue JT, Kemp G, Low D, Quinones-Garcia I. 2003. Evaluation of protein-A chromatography media. J Chromatogr A 989:139–153.

Roque ACA, Lowe CR. 2005. Advances and applications of de novo designed affinity ligands in proteomics. Biotechnol Adv 24:17–26.

Roque AC, Lowe CE, Taipa MA. 2004. Antibodies and genetically engineered related molecules: Production and purification. Biotechnol Prog 20(3):639–654.

Staby A, Holm Jensen I. 2001. Comparison of chromatographic ionexchange resins: II. More strong anion-exchange media. J Chromatogr A 908:149–161.

Staby A, Johansen N, Wahlstrom H, Mollerup I. 1998. Comparison of loading capacities of various proteins and peptides in culture medium and pure state. J Chromatogr A 827(2):311–318.

Staby A, Sand MB, Hansen RG, Jacobsen JH, Andersen LA, Gerstenberg M, Bruus UK, Jensen IH. 2004. Comparison of chromatographic ionexchange resins: III Strong cation-exchange resins. J Chromatogr A 1034:85–97.

Subramanian A, Hommerding J. 2005. The use of confocal laser scanning microscopy to study the transport of biomacromolecules in a macroporous support. J Chromatogr B 818:89–97.

Teske CT, Schroeder M, Simon R, Hubbuch J. 2005. Protein labeling effects in confocal laser scanning microscopy. J Phys Chem B 109:13811–13817.

Thömmes J. 1999. Investigations on protein adsorption to agarose-dextran composite media. Biotechnol Bioeng 62(3):358–362.

Van Oostvelt P, Bauwens S. 1990. Quantitative fluorescence in confocal microscopy. The effect of the detection pinhole on the re-absorption and inner filtering phenomena. J Micros 158:121–132.

Willems A, Leoen J, Schoonooghe S, Grooten J, Mertens N. 2003. Optimizing expression and purification from cell culture medium of trispecific recombinant antibody derivatives. J Chromatogr B 786:161–176.

Wlad H, Ballagi A, Bouakaz L, Gu Z, Janson J-C. 2001. Rapid two-step purification of a recombinant mouse Fab fragment expressed in Escherichia coli. Protein Expr Purif 22(2):325–329.

Zhang X, Grimes BA, Wang J-C, Lacki KM, Liapis AI. 2004a. Analysis and parametric sensitivity of the behavior of overshoots in the concentration of charged adsorbate in the adsorbed phase of charged adsorbent particles: Practical implications for separations of charged solutes. J Colloid Interf Sci 273:22–38.

Zhang X, Wang J-C, Lacki KM, Liapis AI. 2004b. Molecular dynamics simulation studies of the transport and adsorption of a charged macromolecule onto a charged adsorbent solid surface immersed in an electrolytic solution. J Colloid Iterf Sci 277:483–498.

Zhang X, Wang J-C, Lacki KM, Liapis AI. 2005a. Molecular dynamics simulation studies of the conformation and lateral mobility of a charged adsorbate biomolecule: Implications for estimating the critical value of the radius of a pore in porous media. J Colloid Iterf Sci 290:373–382.

Zhang X, Wang J-C, Lacki KM, Liapis AI. 2005b. Construction of molecular dynamics modeling and simulations of the porous structures formed by dextran polymer chains attached on the surface of the pores of a base matrix: Characterization of porous structures. J Phys Chem 109:21028–21039.

Zhou X-P, Li W, Shi Q-H, Sun Y. 2006. Analysis of mass transport models for protein adsorption to cation exchanger by visualization by confocal laser scanning microscopy. J Chromatogr A 1103:110–117.

DOI 10.1002/bit